JOURNAL OF MATERIALS SCIENCE 30 (1995) 3598–3602

Metastability of the K_2NiF_4 type structure of the solid solution $LaCa(Cr_xAl_{1-x})O_4 (0 \leqslant x \leqslant 0.10)$

I. ZVEREVA, L. ZUEVA
Department of Inorganic Chemistry, Chemical Institute, St Petersburg University, 198904 Petrodvorets, St Petersburg, Russia
J. CHOISNET
Centre de Recherche sur la Matière Divisée, UMR CNRS Université, Cristallochimie, Faculté des Sciences, Université d'Orléans, F45067 Orléans Cedex 2, France

Metastability of the K_2NiF_4 type aluminate $LaCaAlO_4$ and its chromium diluted solid solution $LaCaCr_xAl_{1-x}O_4$ ($x \leqslant 0.10$) was evidenced at 1400 °C in air, in terms of demixing into the parent structures of the 1:1 intergrowth, i.e. the perovskite and rocksalt type $LaAlO_3$ ($LaCr_xAl_{1-x}O_3$) and CaO, respectively. This behaviour is discussed comparatively with $YCaAlO_4$ and $LaSrAlO_4$ whose structures are stable under the same thermodynamic conditions. The results of a structure analysis are used to emphasize the role of the nine-fold co-ordination of the ($A^{3+} = Y^{3+}$, La^{3+}; $A^{2+} = Ca^{2+}$, Sr^{2+}) cations as "mixing" the twelve-fold co-ordination of A^{3+} in $A^{3+}AlO_3$ perovskite and the six-fold one of A^{2+} in $A^{2+}O$ rocksalt. Calcium–oxygen underbonding in the (La, Ca)–O–Al bridge is assumed to trigger the metastability of the intergrowth structure at high temperature.

1. Introduction

The existence of the K_2NiF_4 type structure of A_2BO_4 mixed oxides sets the problem of the crystal chemical constraints originating in the 1:1 intergrowth of the AO rocksalt (RS) and ABO_3 perovskite (P) layers (Fig. 1): purely geometrical considerations point to the difficulty in solving properly the adaptability of these layers [1]. For the series of aluminates $YCaAlO_4$, $LaCaAlO_4$, $LaSrAlO_4$, [2–4] these constraints are assumed to depend mainly on steric and chemical effects related to the simultaneous presence of A^{3+} = Y or La and A^{2+} = Ca or Sr cations in the RS layers.

In the following, are reported the thermal behaviour of these aluminates at 1400 °C, which evidences a metastability of $LaCaAlO_4$ and of the diluted chromium solid solution $LaCaCr_xAl_{1-x}O_4$ ($x \leqslant 0.10$), as well. Under the same thermodynamic conditions, $YCaAlO_4$ and $LaSrAlO_4$, together with their diluted chromium solid solutions, are stable. The understanding of such a behaviour is proposed on the basis of a structural analysis of $LaCaAlO_4$, which is discussed comparatively with $YCaAlO_4$ and $LaSrAlO_4$. Specificity of the nine-fold co-ordination of the (A^{3+}, A^{2+}) cations is emphasized, in terms of "mixing" the twelve-fold and six-fold co-ordination of A^{3+} in $AAlO_3$ (P) and A^{2+} in AO (RS), respectively. From this, it is further reported that enhancement of unstability of the (La,Ca)–O–Al bridge bond, which ensures the connection of an (AlO_6) octahedron and an (A–O_9) polyhedron in the intergrowth (Fig. 1), is likely to be due to Ca–O bonding in $LaCaAlO_4$, as compared to the case of the RS structure.

2. Experimental procedure

The synthesis of $LaCaAlO_4$ and of the diluted solid solution $LaCaCr_xAl_{1-x}O_4$ ($x = 0.05$, 0–10) was carried out by the usual solid state methods, i.e. from mixtures of $CaCO_3$, La_2O_3, Al_2O_3 and Cr_2O_3 heated in air, in alumina crucibles. After a progressive increase of the temperature up to 1400 °C, successive annealings for 5 h at this temperature were repeated four times. After each step, the progress of solid state reactions was checked by X-ray powder diffraction.

Crystallographic characterization, cell parameters and structure calculations, was performed for $LaCaAlO_4$ from X-ray powder diffractograms, using a Siemens D-500 diffractometer (CuK_α) to collect 2θ diffraction angles and intensity data which were used in a least square refinement calculation procedure [5].

3. Results and discussion

3.1. Thermal stability of the diluted solid solution $LaCaCr_xAl_{1-x}O_4$ ($x = 0$; 0.05; 0.10)

The compositions ($x = 0$; 0.05; 0.10) of the solid solution $LaCaCr_xAl_{1-x}O_4$ were obtained as pure K_2NiF_4 type phases after two 5 h annealings at 1400 °C. Further annealings for 5 h evidence the progressive appearance of the perovskite type $LaAlO_3$ phase, whose amount regularly increases as the annealings at 1400 °C are repeated. The metastability of the diluted solid solution $LaCaCr_xAl_{1-x}O_4$ further proved to be a specific property of this crystal–chemical system. As a matter of fact, the K_2NiF_4 type structure of the phases $YCaAlO_4$ and $LaSrAlO_4$, and their chromium

0022–2461

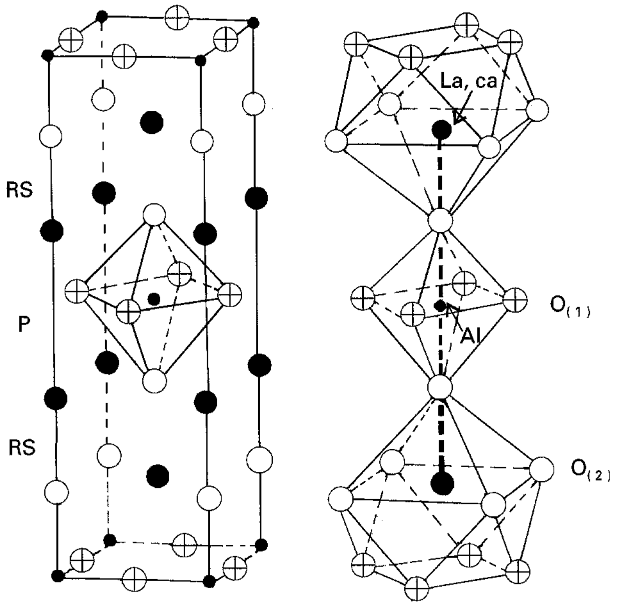

Figure 1 K_2NiF_4 type structure: perovskite (P)–rocksalt (R) 1:1 intergrowth and connection of the (La, Ca) nine-fold co-ordination polyhedron and the (AlO_6) octahedron.

TABLE I Atomic parameters (S.G.I4/mmm) of the K_2NiF_4 type structure of $LaCaAlO_4$: $RI = \Sigma|I_o - I_c|\Sigma I_o = 0.049$

(La, Ca)	Al	$O_{(1)}$	$O_{(2)}$
4(e)	2(a)	4(e)	4(e)
0	0	0	0
0	0	1/2	0
$z = 0.3580(1)$	0	0	$z = 0.1648(4)$
$B(\text{nm})^2$ 0.035(2)	0.060(6)	0.11(1)	0.12(2)

TABLE II Metal oxygen distances (nm) in the $(Al–O_6)$ octahedra and $(A–O_9)$ polyhedra for the K_2NiF_4 type structure of the series of aluminates $A^{3+}A^{2+}AlO_4(A^{3+}, A^{2+}$ = Y, Ca; La, Ca; La, Sr)

Metal–oxygen distances	$YCaAlO_4$	$LaCaAlO_4$	$LaSrAlO_4$
$Al–O_6$ octahedra			
Equal $Al–O_{(1)} \times 4$	0.1822	0.1856	0.1878
Apical $Al–O_{(2)} \times 2$	0.1993(6)	0.2031(5)	0.1997(6)
$A–O_9$ polyhedra			
Out of plane			
$A–O_{(1)} \times 4$	0.2484(1)	0.2551(1)	0.2593(1)
In plane $A–O_{(2)} \times 4$	0.2595(2)	0.2640(2)	0.2664(2)
Apical $A–O_{(2)} \times 1$	0.2256(6)	0.2381(5)	0.2531(6)

diluted solid solutions as well, do not exhibit such a tendency to dissociation in the P and RS structures of $YAlO_3$ and CaO, and $LaAlO_3$ and SrO, respectively. $YCaAlO_4$ and $LaSrAlO_4$ exist as unique phases, even after annealing for 30 h at the temperature of synthesis (1400–1420 °C). The same kind of result is obtained for the mixed lanthanum–yttrium diluted chromium solid solution $Y_{1/2}La_{1/2}CaCr_xAl_{1-x}O_4$, i.e. an homogeneous K_2NiF_4 type structure is saved after 30 h heating at 1400 °C.

3.2. Structure calculations

It was decided to investigate the structure of $LaCaAlO_4$ in order to tentatively evidence some particularity of the interatomic distances. This was done comparative to the results previously obtained by the authors for $YCaAlO_4$ both at room temperature and 1000 °C [2, 6] and for $LaSrAlO_4$ whose structural calculations were performed simultaneously [7].

The details of the procedure which is based on least square refinement calculations [5], were reported in the case of $YCaAlO_4$ [2]. The values of the z coordinates of the A and Al elements, respectively, obtained after minimizing the reliability factor for the intensities, RI, equal to $\Sigma|I_o - I_c|/\Sigma I_o$, are reported in Table I, together with the other variable parameters, namely the four isotropic thermal factors $B(A)$, $B(\text{Al})$, $B(O_1)$, $B(O_2)$.

The metal–oxygen distances both in the $(Al–O_6)$ octahedra and $(La, Ca–O_9)$ polyhedra, as compared to those found for the isotypic phases $YCaAlO_4$ and $LaSrAlO_4$ (Table II), are consistent with the prediction to be deduced from the variation of ionic radii, r, i.e. $r(La^{3+}) > r(Y^{3+})$ and $r(Ca^{2+}) < r(Sr^{2+})$: the mean size of the $(La, Ca–O_9)$ polyhedra is intermediate between that of $(Y, Ca–O_9)$ and $(La, Sr–O_9)$ polyhedra, with the occurrence of a short apical $(La, Ca)–O_2$ distance close to 0.238 nm. Still, one feature seems to be surprising: the apical $Al–O_2$ distance, close to 0.203 nm, shows up an increase with respect to the nearly unchanged values obtained for $YCaAlO_4$ and $LaSrAlO_4$: 0.1993 nm and 0.1997 nm. This will be further emphasized in the following discussion, as directly connected to the problem of the unstability of the mixed (La, CaO) RS layer.

3.3. Metastability of $LaCaAlO_4$: a crystal–chemical approach

3.3.1. Geometrical considerations

A usual way of modelling the geometrical factors which account for the existence of the perovskite structure of an ABO_3 oxide consists in calculating the tolerance factor [8] defined as $t = (rA^{n+} + rO^{2-})/[2(rB^{p+} + rO^{2-}]^{1/2}$. The tolerance factor can be considered as a measure of the adaptability of an octahedral layer with an AO plane, this one being a typical $\{100\}$ plane of the RS structure.

Such modelling can be extended to the 1:1 intergrowth of an octahedral layer and an RS layer, on the basis of nine-fold co-ordination of the A cations, instead of a twelve-fold one in the perovskite structure. Table III reports the set of values of t, namely t(P/RS) for the intergrowth structure and t(P) for the perovskite structure, calculated for the series of K_2NiF_4 type aluminates $A^{3+}A^{2+}AlO_4$ (A^{3+} = Y, La; A^{2+} = Ca, Sr), and the perovskite type aluminates $YAlO_3$ and $LaAlO_3$, from one part and for the series of corresponding 10% chromium containing solid solutions, from another part. The comparison between these values is made in terms of the deviations Δt|(P/RS) – (P)|.

The most significant deviation, Δt(P/RS) – (P) = 0.030, when building the P/RS intergrowth of an $A^{3+}A^{2+}AlO_4$ phase from $A^{3+}AlO_3$ (P) and $A^{2+}O$

TABLE III Tolerance factors calculated for P/RS intergrowth type $A^{3+}A^{2+}\mathrm{AlO_4}$ phases (A^{3+}, A^{2+} = Y, Ca; $\mathrm{Y_{1/2}La_{1/2}}$, Ca; La, Ca; La, Sr) perovskite type (P) $A^{3+}\mathrm{AlO_3}$ phases (A^{3+} = Y, $\mathrm{Y_{1/2}La_{1/2}}$, La) and the corresponding 10% chromium containing solid solutions and deviations $\Delta t|(\mathrm{P/RS}) - (\mathrm{P})|$

Formula	Al	$\mathrm{Cr_{0.1}Al_{0.9}}$
For t (P/RS)		
$\mathrm{YCa(\ )O_4}$	0.953	0.949
$\mathrm{Y_{1/2}La_{1/2}Ca(\ )O_4}$	0.962	0.958
$\mathrm{LaCa(\ )O_4}$	0.972	0.967
$\mathrm{LaSr(\ )O_4}$	0.994	0.989
For t (P)		
$\mathrm{Y(\ )O_3}$	0.968	0.964
$\mathrm{Y_{1/2}La_{1/2}(\ )O_3}$	0.985	0.981
$\mathrm{La(\ )O_3}$	1.002	0.997
$\mathrm{La(\ )O_3}$	1.002	0.997
$\Delta t|(\mathrm{P/RS}) - (\mathrm{P})|$		
$\mathrm{YCa(\ )O_4}$	0.015	
$\mathrm{Y_{1/2}La_{1/2}Ca(\ )O_4}$	0.023	
$\mathrm{LaCa(\ )O_4}$	0.030	
$\mathrm{LaSr(\ )O_4}$	0.008	

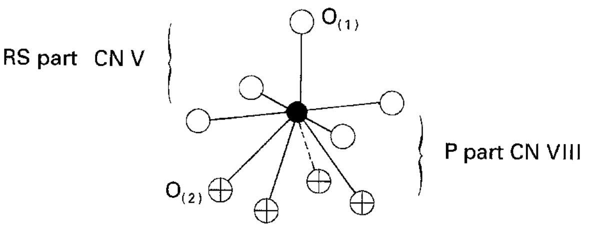

Figure 2 Analysis of the nine-fold co-ordination of the A element in terms of an eight-fold perovskite (P) part and a five-fold rocksalt (R) part.

TABLE IV Analysis of the nine-fold co-ordination of the A cations in the P/RS intergrowth in terms of a P part and an RS part (distance in nm)

	$\mathrm{YCaAlO_4}$	$\mathrm{LaCaAlO_4}$	$\mathrm{LaSrAlO_4}$
P part			
$d(A^{3+}, A^{2+}\text{–O})$	0.2540	0.2596	0.2628
CN VIII	0.291[a] 0.240[b]	0.268[c]	0.268[c]
RS part			
$d(A^{3+}, A^{2+}\text{–O})$	0.2527	0.2588	0.2638
CN V	0.240[d]	0.240[d]	0.257[e]

[a] d $\mathrm{Y^{3+}}$–O calculated for the twelve-fold co-ordination in $\mathrm{YAlO_3}$ [9].

[b] d $\mathrm{Y^{3+}}$–O calculated for the eight nearest oxygen neighbours in $\mathrm{YAlO_3}$ [9].

[c] d $\mathrm{La^{3+}}$–O observed for the twelve-fold co-ordination in $\mathrm{LaAlO_3}$ [10].

[d] d Ca–O observed for the octahedral co-ordination in CaO [11].

[e] d Sr–O observed for the octahedral co-ordination in SrO [11].

(RS) is observed for the pair "La, Ca". The nearly perfect adaptability of an octahedral (Al–O) layer with a LaO plane, which exists in $\mathrm{LaAlO_3}$, is damaged by the participation of CaO to the RS layer in the P/RS intergrowth of $\mathrm{LaCaAlO_4}$. Such a geometrical constraint, as measured by $\Delta t|(\mathrm{P/RS}) - (\mathrm{P})|$, is progressively lowered in the series "$\mathrm{Y_{1/2}La_{1/2}Ca}$", "Y,Ca", and further decreased when considering the pair "La, Sr", which exemplifies a slight constraint in the P/RS intergrowth. These data can be assumed to be unchanged when considering the corresponding 10% chromium solid solutions.

A progress in the understanding of the problems of adaptability of an octahedral layer with a RS layer can be obtained if one thinks of the specificity of the nine-fold co-ordination of the A cations in the P/RS intergrowth. In the $A^{3+}A^{2+}\mathrm{AlO_4}$ phases, the nine-fold co-ordination results from "mixing" the twelve-fold co-ordination of A^{3+} in $A\mathrm{AlO_3}$(P) and the six-fold octahedral co-ordination of A^{2+} in AO (RS). From this analysis, it is possible to calculate in the P/RS intergrowth, the mean (A^{3+}, A^{2+}–O) distance corresponding to eight oxygen neighbours out of twelve in the P structure, i.e. the P part of the nine-fold co-ordination and the mean (A^{3+}, A^{2+}–O) distance corresponding to five oxygen neighbours out of six in the RS structure, i.e. the RS part of the nine-fold co-ordination (Fig. 2 and Table IV).

First of all, the P part and the RS part of the nine-fold co-ordination of the A cations, as modelled by these mean distances, are very similar. This geometrical data of the nine-fold co-ordination, up to now never emphasized, is supposed to be a typical property of the $\mathrm{K_2NiF_4}$ type structure. This will be further analysed in this way in a forthcoming paper. As a consequence, the nearly excellent equilibrium between the components of the nine-fold co-ordination of the A cations, is in no way at the source of whatever kind of instability effects the P/RS intergrowth. Nevertheless, it is very informative to understand how such an equilibrium is reached for the three aluminates under question, i.e. to compare each part of the nine-fold co-ordination with its parent co-ordination in the P and RS structures, respectively (Table IV). In this respect, the following statements can be proposed

1. $\mathrm{LaSrAlO_4}$ is unambiguously the most stable P/RS intergrowth, on the basis of the rather small deviation of the La–O distance in the intergrowth and in $\mathrm{LaAlO_3}$ from one part, and of the Sr–O distance in the intergrowth and Sr–O from another part. In such a case, the adaptability of the P and RS structures is ensured without any significant distortion in the geometrical characteristics of the co-ordination of A cations.

2. $\mathrm{YCaAlO_4}$ shows a stable P/RS intergrowth mainly depending on an improvement of the stability of the P slab. As a matter of fact, the eight-fold P part of the co-ordination is closer to the usual oxygen co-ordination of $\mathrm{Y^{3+}}$ than the strongly distorted twelve-fold co-ordination in $\mathrm{YAlO_3}$ [10] which is better understood in terms of eight nearest neighbours. Otherwise, the RS part of the co-ordination evidences a rather large deviation of the Ca–O distance with respect to CaO.

3. $\mathrm{LaCaAlO_4}$ focuses in its P/RS intergrowth instabilities both on the P and the RS parts. If these phenomena can be considered as not so crucial for the La–O distances in the P part, the situation is different in the RS part where the Ca–O distances are nearly 0.019 nm longer than in CaO (Table IV). Under these

conditions, it is not so surprising that at 1400 °C, on the basis of a further lengthening of the Ca–O distances, a similar effect was previously evidenced by a structural study of $YCaAlO_4$ at 1000 °C [6], the stability of the P/RS intergrowth vanishes and the parent phases, $LaAlO_3$ and CaO, progressively take the place of $LaCaAlO_4$.

3.3.2. Evidence of calcium–oxygen underbonding

The geometrical data can be further used to emphasize some particularity of the A–O(A^{3+}, A^{2+}) and Al^{3+}–O bonds in the P/RS intergrowth, namely in the A-$O_{(2)}$–Al bridge. Such considerations aim to obtain a qualitative comparison of these bonds in the series $YCaAlO_4$, $LaCaAlO_4$, $LaSrAlO_4$ with respect to parent bonding in $A^{3+}AlO_3$ (A^{3+} = Y, La) P phases and the $A^{2+}O$ (A^{2+} = Ca, Sr) RS phases. By lack of any knowledge of the ionic and covalent contributions to the metal–oxygen bonding, as modelled from the results of quantum chemical calculations in the K_2NiF_4 type structure of La_2NiO_4 and La_2CuO_4 [12], a detailed analysis of the problems of bonding cannot be proposed. Still, these typical problems, as systematically related to the geometrical constraints originating in building the P/RS intergrowth, which are reported above, refer to the same kind of modelling. In this respect, the statements that Brown reported in his modelling of the crystal–chemical constraints of La_2NiO_4 [1, 13] can be used presently as a basis for a discussion of the stability of the A–O and Al–O bonds. Therefore, as a consequence of the adaptability of the P and RS structures to be solved properly, i.e. to obtain a ratio: in plane A–$O_{(2)}$ distances over equatorial Al–$O_{(1)}$ distances (Table II) as close as possible to $2^{1/2}$, this is well observed in the series $YCaAlO_4$: 1.424; $LaCaAlO_4$: 1.422; $LaSrAlO_4$: 1.419, there is significant compression of the four equatorial Al–$O_{(1)}$ distances coupled with a stretching of the in plane A–$O_{(2)}$ distances. This co-operative effect results in equatorial Al–$O_{(1)}$ overbonding and in plane A–$O_{(2)}$ underbonding.

One can think of several crystal–chemical mechanisms to be able to relax these strains, as discussed for La_2NiO_4 [13]: some are more chemical and only one is purely geometrical. The chemical mechanisms are precluded for this series of aluminates; as a matter of fact, in no way is the occurrence of supplementary interstitial oxygen as in $La_2NiO_{4+\delta}$ [14] nor can a coupled deficiency of A and O like in $La_{2-x}NiO_{4-x}$ [15] be considered. The only way to solve the strain on the equatorial Al^{3+}–$O_{(1)}$ and in plane A–$O_{(2)}$ bonding is found in a shift of the $O_{(2)}$ apical oxygen towards the A cations: clearly, this is the case of these aluminates, as deduced from the values of the apical A–$O_{(2)}$ and Al^{3+}–$O_{(2)}$ distances (Table II). The co-operative lengthening–shortening of the apical dAl–$O_{(2)}$ and dA–$O_{(2)}$ distances, respectively, aims to compensate the coupled equatorial Al–$O_{(1)}$ overbonding, in a plane A–$O_{(2)}$ underbonding, originating in the proper geometrical adaptability of the P and RS structures, as described above.

The comparison of these co-operative bonding effects for the three aluminates points to a regular decrease of the equatorial Al–$O_{(1)}$ overbonding in the series $YCaAlO_4$, $LaCaAlO_4$, $LaSrAlO_4$, increase of the corresponding distances (Table II), which get closer to the mean value of dAl–O in octahedral co-ordination, i.e. 0.193 nm. As regards the A–$O_{(2)}$ bonding, $LaCaAlO_4$ shows a specific behaviour which can be analysed in the following terms

1. The in plane A–$O_{(2)}$ underbonding is the largest for $LaCaAlO_4$; as connected to the big difference between the corresponding distances: 0.264 nm and the mean value of dCa–O in octahedral co-ordination, i.e. 0.24 nm.
2. The increase of the in plane Ca–$O_{(2)}$ underbonding in $LaCaAlO_4$ is not satisfactorily balanced by a corresponding increase of the apical Ca–$O_{(2)}$ overbonding; 0.238 nm, is only slightly lower than the Ca–O distance, 0.24 nm.
3. An enhancement of the problems of underbonding in $LaCaAlO_4$ can be found in the Ca–$O_{(2)}$–Al bridge, which ensures connection of the P and RS layers in the P/RS intergrowth. As the apical Al–$O_{(2)}$ distance, 0.203 nm, is larger than in both $YCaAlO_4$ and $LaSrAlO_4$, 0.1993 and 0.1997 nm, respectively, the weakening of the co-operative apical Ca–$O_{(2)}$ and Al–$O_{(2)}$ bonds of the Ca–$O_{(2)}$–Al bridge is maximum in $LaCaAlO_4$.

From this, the main contribution to the metastability of the P/RS intergrowth of $LaCaAlO_4$ is to be found in an overall calcium–oxygen underbonding. In this respect, the Ca–$O_{(2)}$–Al bridge plays a particular role, as such bonding is not strong enough to prevent at high temperature a separation between the P and RS components of the intergrowth in terms of demixing in $LaAlO_3$ (P) and CaO (RS) parent oxides.

4. Conclusions

The metastability of the K_2NiF_4 type structure of $LaCaAlO_4$ and its diluted chromium solid solution $LaCa(Cr_xAl_{1-x})O_4$ ($x \leqslant 0.10$) brings a typical example of enhancement of the crystal–chemical constraints on which depend the existence of the 1:1 intergrowth of ABO_3 perovskite and AO rocksalt phases. As compared to $YCaAlO_4$ and $LaSrAlO_4$, $LaCaAlO_4$ focuses instabilities both on the P and RS parts of its intergrowth. In this respect, evidence of calcium–oxygen underbonding was obtained from the results of a structural analysis: this is very likely to play a main role in the demixing process observed when heating for more than 10 h at 1400 °C. This feature is of particular importance for the solid solution, because the equilibrium state of the distribution of the paramagnetic Cr^{3+} ions in the P layer can be reached only after long annealings, 30 h at least, as proved for the $YCaCr_xAl_{1-x}O_4$ solid solution [2]. Consequently, for the $LaCaCr_xAl_{1-x}O_4$ solid solution, due to the metastability of its intergrowth structure at high temperature, it is not possible to reach such an equilibrium state for the distribution of the Cr^{3+} ions.

More generally, the specific behaviour of the pair "La, Ca" in the aluminates and aluminochromites, in terms of triggering rather easily a metastability of the P/RS intergrowth of the K_2NiF_4 type structure, is well related to other crystal–chemical data; as an example, for the K_2NiF_4 type nickelates $La_{2-x}Ca_xNiO_{4-\delta}$, the $x = 1$ composition, i.e. $LaCaNiO_{4-\delta}$ does not exist as a pure phase [16].

References

1. I. D. BROWN, *Acta Cryst.* **B48** (1992) 553.
2. F. ARCHAIMBAULT, J. CHOISNET and I. ZVEREVA, *Mater. Chem. Phys.* **34** (1993) 300.
3. Y. P. OUDALOV, A. DAOUDI, J. C. JOUBERT, G. LE FLEMM and P. HAGENMULLER, *Bull. Soc. Chem. Fr.* **10** (1970) 3408.
4. F. GANGULI and C. N. R. RAO, *J. Solid State Chem.* **53** (1984) 193.
5. C. C. PHAM, J. CHOISNET and B. RAVEAU, *Bull. Acad. R. Belg. Cl. Sci.* **61** (1975) 473.
6. J. CHOISNET, F. ARCHAIMBAULT, M. CRESPIN, N. CHEZINA and I. ZVEVERA, *Eur. J. Solid State Inorg. Chem.* **30** (1993) 619.
7. J. CHOISNET and I. ZVEREVA, unpublished data.
8. A. F. WELLS, "Structural Inorganic Chemistry" (Oxford University Press, 1984) p. 586.
9. R. DIEHL and G. BRANDT, *Mater. Res. Bull.* **10** (1975) 85.
10. S. GELLER and V. B. BALA, *Acta Cryst.* **9** (1019) 1956.
11. W. HÜCKEL, "Structural Chemistry of Inorganic Compounds" (Elsevier, Amsterdam, 1951) p. 123.
12. J. CHOISNET, R. A. EVARESTOV, I. I. TUPITSIN and V. A. VERYAZOV, *Phys. Status. Solidi B* **179** (1993) 441.
13. I. D. BROWN, *Z. Kristallogr.* **199** (1991) 255.
14. J. D. JORGENSEN, B. DABROWSKY, SHIYOU PEI, D. R. RICHARDS and D. G. HINKS, *Phys. Rev.* **B40** (1989) 2187.
15. J. CHOISNET, J. M. BASSAT, H. PILLIERE, P. ODIER and M. LEBLANC, *Solid State Comm.* **66** (1988) 1245.
16. D. CORRIGNAN, Diploma, University of Orléans (1986).

Received 31 May 1994
and accepted 20 January 1995